EJN
European Journal of Neuroscience

European Journal of Neuroscience, Vol. 27, pp. 2773–2780, 2008 doi:10.1111/j.1460-9568.2008.06219.x

Anisotropy in the representation of direction preferences in cat area 18

Jérôme Ribot,* Shigeru Tanaka, Kazunori O'Hashi and Ayako Ajima†
Laboratory for Visual Neurocomputing, RIKEN Brain Science Institute, Hirosawa 2–1, Wako-shi, Saitama 351–0198, Japan

Keywords: area 18, direction selectivity, optic flow, optical imaging, visual system

Abstract

Higher visual cortical areas are involved in the perception of complex stimuli, such as the optic flow created by self-motion. On the other hand, area 18 is thought to extract primitive visual features, feeding higher cortical areas for further processing. In this study, we applied optical imaging of intrinsic signals in the central, lower visual field of cat area 18, and reconstructed direction preference and direction selectivity maps in each hemisphere. We observed a significant overrepresentation of downward and temporal directions, in accordance with previous electrophysiological results. Cardinal orientations were not overrepresented, however. Downward directions were overrepresented at the highest direction selectivity domains. Temporal direction representation, on the other hand, decreased with direction selectivity. Our findings therefore suggest the existence of a neural substrate for the processing of optic flow in cat area 18.

Introduction

Navigating through the environment requires the integration of various dynamic elements. The optic flow associated with self-motion is of particular interest as it carries stereotyped information that could be used for visual guidance and obstacle avoidance (Gibson, 1954; for review see Sherk & Fowler, 2001). This pattern of motion typically exhibits two particular components that are expected to be detected in higher visual areas (Koenderink, 1986): a strong radial component directed outward from the heading point, and curved components that also depend on the observer's direction of motion (Fig. 1A).

In cat visual cortex, several experiments have implicated lateral suprasylvian areas in the processing of such stimuli (Hamada, 1987; Rauschecker *et al*., 1987; Sherk *et al*., 1995; Brosseau-Lachaine *et al*., 2001). Area 18, on the other hand, is more commonly regarded as an array of linear detectors involved in basic visual measurements, such as the local detection of orientated edges and movement directions. Still, in area 18, unit recordings have revealed an anisotropic distribution of preferred directions (Berman *et al*., 1987; Bauer *et al*., 1989) that could reflect the existence of a neural substrate for the processing of self-motion. Typically, these studies focused on a cortical region located at the surface of the cortex, which retinotopically corresponded to only part of the lower, central visual field (Fig. 1B). In this region of interest, the expansion of the optic flow is restricted to downward and temporal directions. Berman *et al*. (1987) found that both downward and temporal directions were overrepresented compared to other directions. Bauer *et al*. (1989), moreover, suggested that such anisotropy might also depend on the depth of the recording sites.

Correspondence: Dr Jérôme Ribot, at *present address below.
E-mail: jerome.ribot@college-de-france.fr

**Current address*: Laboratoire de Physiologie de la Perception et de l'Action, UMR 9950, Collège de France–CNRS, 11 Place Marcelin Berthelot, 75005 Paris, France.

†*Current address*: Laboratory for Vocal Behaviour Mechanisms, RIKEN Brain Science Institute, as above.

Received 2 May 2007, revised 19 March 2008, accepted 19 March 2008

These two studies (Berman *et al*., 1987; Bauer *et al*., 1989) are based on single-unit recording studies, and have suggested that there is a biased distribution of direction preferences among cells in area 18. However, single-unit recording suffers from problems of biased sampling because cells are grouped to some degree in a columnar fashion according to preferred direction. In this study we used optical imaging (Bonhoeffer & Grinvald, 1991) in order to assess direction preference; this method is better suited for collection of a large and unbiased sample of direction preference across area 18. Neurons that share similar preferred directions tend to be organized into vertical columns in superficial layers of area 18 (Berman *et al*., 1987; Swindale *et al*., 1987). Their tangential visualization has revealed almost continuous representation of preferred directions except along fractures, at which preferred directions abruptly change by 180° (Shmuel & Grinvald, 1996; Weliky *et al*., 1996). We took advantage of this technique and investigated how the cortical territory devoted to cardinal directions was represented in cat area 18.

Materials and methods

The present experimental protocol was approved by the Institutional Animal Research Committee of RIKEN (Nos. H13-B040 and H17-2B043), and surgical procedure and optical imaging were performed in accordance with the 'Guiding Principles for the Care and Use of Animals in the Field of Physiological Science' of the Japanese Physiological Society.

We applied optical imaging of intrinsic signals in 20 cats aged from postnatal 80 days to 8 years (median 144 days), and reared under normal visual conditions (16-h light, 8-h dark cycle).

Surgical procedure

Initial anaesthesia was induced with ketamine hydrochloride (7.0 mg/kg, i.m.), followed by sedation with medetomidine hydro-

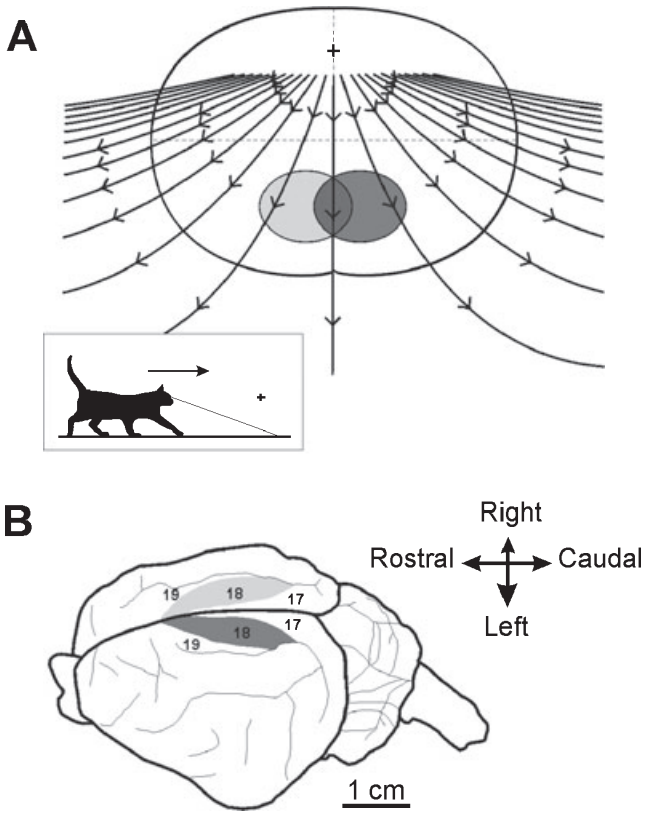

FIG. 1. Optic flow generated by forward locomotion and relationship with the recorded area. (A) Schematic representation of the motion field created by forward locomotion when the cat's gaze was constant and directed downward, close to the midsagittal plane (adapted from Sherk & Fowler, 2001). The cross indicates the heading direction. The black contour corresponds to the cat's visual field limits. Note that the lines of motion created by forward locomotion in the lower-left visual field (light grey) and the lower-right visual field (dark grey) are symmetrical with respect of the vertical meridian. (B) Anatomical representation of the accessible area 18 for the use of optical imaging (adapted from Tusa *et al*., 1979). Dark grey region (left hemisphere) and light grey region (right hemisphere), respectively, represent part of the lower-right and lower-left visual fields in A.

chloride (0.06–0.1 mg/kg, i.m.). The animals were fixed in a stereotaxic apparatus and subsequently artificially ventilated with a 3 : 2 mixture of N_2O and O_2 containing 0.5–1.0% isoflurane. Heart rate, end-tidal CO_2 concentration and rectal temperature were continuously monitored and maintained within normal limits during surgery (120–150 cycles/min, 3.0–4.0% and 37–39°C, respectively). A chamber made of dental cement was mounted on the skull and anchored with stainless steel screws. Then the skull and dura mater covering the recording area were removed. The cranial window (17 × 12 mm) was positioned approximately from P5 to A12, and straddled the midline. The chamber was then filled with 2% agar containing gentamicin sulphate (0.4 mg/mL) and dexamethasone sodium phosphate (0.16 mg/mL), and sealed with a thin film of polyvinylidene chloride to protect against bacterial infection. Finally, the chamber was covered with a plastic artificial skull to protect the brain from mechanical damage. According to the report by Tusa *et al.* (1979), the retinotopic location of our region of interest typically ranges from 5° ipsilateral to ∼20° contralateral in the azimuth, and from slightly lower than the horizontal meridian to −30° in the elevation.

Optical imaging

Animals were artificially ventilated and anaesthetized as in surgery, and paralysed with pancuronium bromide (0.1 mg/kg/h). The cortex was illuminated with a light of 700 nm wavelength. Heart rate, end-tidal CO_2 concentration, and rectal temperature were maintained within normal limits as in surgery. The focal plane was adjusted to 500 μm below the cortical surface using a tandem-lens macroscope arrangement. The optic discs were plotted by tapetal reflection on a paper sheet covering a tangent screen placed 30 cm in front of the animal. The centre of the screen was chosen 8 cm (∼ 15°) below the middle of the two optic discs, that is, ∼8.5° in the lower visual field of the animal (Bishop *et al*., 1962). Intrinsic optical signals were measured while the animals were exposed to visual stimuli displayed on a CRT monitor placed 30 cm in front of the animal. The size of the display was ∼75 × 56° of visual angle. The image had a resolution of 11 pixels/° and the refresh rate was 120 Hz.

Images of cortical activity were obtained with a CCD video camera and digitized and stored using IMAGER 3001 (Optical Imaging Inc., New York, USA). The intrinsic optical signal in response to each stimulus was recorded immediately after the stimulus onset. Five frames of 1 s duration each were recorded. Only the last 3 s, which correspond to the strongest intrinsic signal, were used for data analysis. Each stimulus was presented once in a pseudo-random sequence in a single trial of recordings, and interleaved with blank-screen presentation for 15 s. Twenty-six trials were collected in each recording session.

Stimulation

Immediately after the surgery, we stimulated the animal with full-screen square-wave gratings with two spatial frequencies of 0.15 (area 18 optimal; Movshon *et al*., 1978) and 0.5 cycle/° (area 17 optimal; Movshon *et al*., 1978), drifting in two directions at six equally spaced orientations. Data were then analysed offline. We functionally identified area 17 as the cortical area activated by the high spatial frequency stimulation (e.g. 0.5 cycle/°; Bonhoeffer *et al*., 1995). Functional area 18 was defined by subtracting functional area 17 from the area activated by low spatial frequency stimulation (e.g. 0.15 cycle/°). All procedures for optical imaging were performed under aseptic conditions for the recovery of the animal.

The second experiment was performed 1 week later. We focused on the identified area 18, typically located at the rostral part of the chamber, and stimulated the animal with full-screen, orientated square-wave gratings with a spatial frequency of 0.15 cycle/°, and drifting at 12 ($n = 14$ hemispheres) or 16 ($n = 21$ hemispheres) equally spaced directions of motion. The temporal frequency of the gratings was fixed at 2.0 Hz. In one additional experiment, we stimulated the animal with fields of randomly positioned dots that moved coherently in eight different directions. Each dot was 0.4° in diameter. The ratio of the area covered by dots to the background was ∼0.12. The density of dots was ∼0.23 dots per degrees^2.

Data analysis

Data of intrinsic signals were processed in three steps: (i) the first-frame analysis (Bonhoeffer & Grinvald, 1996) was applied to the recorded data first; (ii) the generalized indicator function method (Yokoo *et al*., 2001) and low-pass filtering were applied next; and (iii) the vector sum method (Blasdel & Salama, 1986; Bonhoeffer & Grinvald, 1991) and Mises function interpolation (Swindale *et al*., 2003) were applied to extract orientation and direction preferences, respectively. Each procedure is detailed in the following paragraphs.

Generally, the baseline of intrinsic signals is uncertain because cortical tissues absorb light even in the absence of any visual stimulus. The first frame of each trial of imaging does not contain intrinsic signals reflecting neural activities in response to visual stimuli because activation of intrinsic signals require 1–2 s from the onset of visual stimulus presentation (Bonhoeffer & Grinvald, 1996). To determine the null response level, in each trial, we subtracted intrinsic signals in the first frame from signals in the subsequent frames in a pixel-by-pixel manner.

Even though the baseline level is determined by the first-frame analysis, intrinsic signals evoked by the presentation of a single stimulus exhibit considerable frame-to-frame variations. These variations are uncontrollable even if we attempt to maintain all experimental parameters constant during imaging. This indicates that observed activity should be treated as a random variable, having some probability distribution. Also, it is reasonable to assume that stimulus-uncorrelated activity is noise. The generalized indicator function method is a novel multivariate analysis technique (Yokoo *et al*., 2001), which identifies the stimulus-related activity patterns (signals), without prior knowledge about the signal and noise characteristics. The extracted signals, that is, the generalized indicator functions, are determined by maximizing the weighted difference between the signal variance and the noise variance. This algorithm efficiently extracts stimulus-related activity patterns from noisy signals originating mainly from blood vessels and spatially slowly varying fluctuations inherent in the recorded signals. In the original generalized indicator function method, the stimulus-related activity pattern was defined as (activity in response to a stimulus) − (activity in response to the cocktail blank). In this study, the definition of stimulus-related activity pattern was given by [(activity in response to a stimulus) − (activity at the first frame)]/(activity at the first frame). This redefinition leads to the signal and noise variations of the optimization function used for the method.

Furthermore, we applied Gaussian low-pass filtering with a 150-μm radius to signals following the application of the generalized indicator function method to eliminate high frequency components of noise. In this way, a single-condition map for each stimulus was reconstructed.

The preferred orientation at each pixel was determined by the use of the vector sum method (Blasdel & Salama, 1986; Bonhoeffer & Grinvald, 1991). We used the Mises function interpolation (Swindale *et al*., 2003) to determine the direction preference and direction selectivity at each pixel. At each pixel, we set the preferred direction φ_{pref} and opposite directions φ_{opp} 180° apart, and reconstructed the direction tuning curve with the use of Mises function interpolation. The model function M as a function of the direction stimulus of motion φ was:

$$M(\varphi) = A_{\mathrm{pref}} \exp\{k_{\mathrm{pref}}[\cos(\varphi - \varphi_{\mathrm{pref}}) - 1]\} + A_{\mathrm{opp}} \exp\{k_{\mathrm{opp}}[\cos(\varphi - \varphi_{\mathrm{opp}}) - 1]\} \quad (1)$$

where A_{pref} and A_{opp} are the heights of the individual peaks at the preferred direction φ_{pref} and opposite direction 180° apart φ_{opp}, respectively. k_{pref} and k_{opp} are inversely related to the widths of each peak. These parameters were adjusted to minimize the goodness of fit f defined as the average square error between the interpolated values $M(\varphi_n)$ and the original data $R(\varphi_n)$:

$$f = \sqrt{\frac{1}{N}\sum_{n=1}^{N}(R(\varphi_n) - M(\varphi_n))^2} \quad (2)$$

This method not only provides a good approximation of the tuning curve at direction-selective pixels, but also discriminates nondirection-selective domains through the rejection of unlikely parameters for the fitting function (A_{pref} or $A_{\mathrm{opp}} < 0$; half-width at half-height < 15°), bad goodness of fitting ($f > 10$), or absence of convergence for the interpolation after 500 iterations. We adopted the same criteria in this study. On average, in our experiments, unselective pixels represented on average 2.0 ± 1.4% standard deviation of the total number of pixels.

At each direction-selective pixel, we defined the direction selectivity index $DS = 1 - M(\varphi^{\mathrm{opp}})/\mathrm{M}(\varphi^{\mathrm{pref}})$ where φ^{pref} and φ^{opp} are the preferred and opposite directions obtained by fitting the model function (Eqn 1) to the data. A value of 0 corresponds to similar response strength at the preferred and opposite directions. A value of 1 indicates that only the preferred direction participates in the establishment of the direction tuning curve.

Statistical analyses were performed with the use of Graphpad PRISM 3.0. The direct comparison between the four cardinal directions' representation was made by applying a one-way repeated-measures ANOVA with the percentage of pixels as the dependent variable, followed by a Bonferroni *post hoc* test. A similar analysis was performed in order to test the robustness of orientation anisotropy.

Results

Significant anisotropy in the representation of direction preferences

In order to test the hypothesis that downward and temporal direction preferences are overrepresented in the lower field representation in area 18, we applied optical imaging of intrinsic signals in area 18 for 20 anaesthetized and paralysed cats, in the right ($n = 19$) and left ($n = 16$) hemispheres.

Fig. 2A shows the single-condition maps in one cat for eight directions of stimulation. Black domains correspond to the intrinsic signal evoked by each stimulus. The magnitude of the signal evoked by downward directions of stimulation was higher than the magnitude of the signal evoked by other directions of stimulation. Differential maps for opposite directions of stimulation are shown in Fig. 2B. From this set of maps, it is more difficult to see any indication of a bias toward any particular directions. The size and signal strength of the patches seem almost equal for each opposite direction. However, domains responding preferentially to downward directions seem larger than domains responding preferentially to upward directions (white patches are larger than dark patches in the third image in Fig. 2B).

We therefore reconstructed direction-preference maps and calculated the histogram of preferences for the cardinal directions (± 45°). Figure 3A shows examples of the maps and histograms. The distribution of preferred directions for the two hemispheres (Fig. 3B, black bars) exhibited a clear peak at the downward direction (One-group t-test, $P < 0.001$). Upward directions, on the other hand, were significantly underrepresented (one-group t-test, $P < 0.001$). In each hemisphere, the increase in the number of pixels representing temporal directions was accompanied by a decrease in the number of pixels representing nasal directions. The cortical territory devoted to each horizontal direction became significantly different between hemispheres (paired t-test, $n = 15$, $P < 0.001$ for both horizontal directions), but the distribution of preferred directions around the upward and downward directions remained unchanged on average (paired t-test, $n = 15$, $P > 0.5$ and $P > 0.9$, respectively). Therefore, horizontal direction representations are best described with reference to the hemisphere.

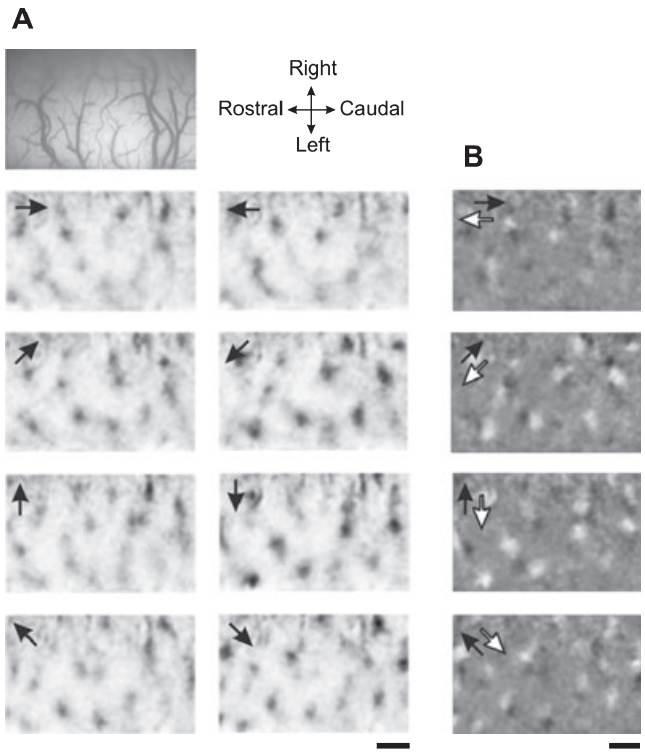

FIG. 2. Optical imaging in area 18 of cat visual cortex. (A) Single-condition maps obtained for eight directions of stimulation. Black domains correspond to the intrinsic signal evoked by each stimulus. (B) Differential maps for pairs of opposite directions of motion. Each differential map was reconstructed by subtracting a single-condition map in response to one direction of motion from a single-condition map in response to the opposite direction of motion. Dark and bright patches in each image represent cortical areas that preferred motion in the direction of the black and white arrows marked on the image, respectively. The maps contain significant portions of grey areas, implying no preference for either of the two directions of motion. Data were obtained from the right hemisphere. Temporal directions therefore correspond to leftward directions. Scale bar, 1 mm.

Fig. 3C summarizes these results, for which directions in one hemisphere have been reversed with respect to the vertical meridian. A one-way repeated-measures ANOVA showed that the anisotropy was highly robust in the 20 cats (Table 1). Bonferroni's *post hoc* test confirmed the overrepresentation of the downward and temporal directions compared to upward and nasal directions ($P < 0.001$). In addition, we found that the cortical territory devoted to downward directions was larger than the cortical territory devoted to temporal directions ($P < 0.001$).

Absence of anisotropy in the distribution of orientation preferences

In addition to direction maps, we also calculated orientation preference maps. Figure 4A shows an example of an orientation preference map and a direction preference map obtained in the same cat. We represented in a scatterplot in Fig. 4B the preferred orientation and the preferred direction of 1000 randomly chosen pixels. We confirmed that orientation and direction preference values tended to be constrained, orthogonal to each other (mean absolute difference 89.7 ± 7.7° over the 20 cats).

It has been reported that, in cat areas 17 and 18, cardinal orientations are overrepresented compared to oblique orientations (Frégnac & Imbert, 1978; Berman *et al*., 1987; Wang, 2004; Imamura *et al*., 2006). Such bias toward cardinal orientations might reflect the preponderance of vertical and horizontal edges in natural scenes (Coppola *et al*., 1998). In particular, in cat area 18, Berman *et al*. (1987) recorded more neurons coding for vertical and horizontal orientations. Because orientation and direction preferences are constrained, we wondered whether the anisotropy in the representation of orientation preferences could affect the anisotropy in the distribution of direction preferences.

Fig. 4C represents the relative distribution of cardinal and oblique orientations in the 20 cats we recorded. We calculated the average cortical area devoted to cardinal and oblique orientations and failed to show any significant anisotropy in the representation of orientation preferences (Table 2). Therefore, despite the fact that the preferred direction of a neuron tends to be orthogonal to its preferred orientation, our results therefore suggest that direction anisotropy can exist independently of orientation anisotropy.

Dependence on direction selectivity

In area 18, direction selectivity varies among different neurons. Figure 5A illustrates the distribution of direction selectivity in optical imaging. Most of the domains exhibited low direction selectivity: almost 90% of the pixels responded to the opposite direction of motion with at least half the strength of the response to the preferred direction (DS < 0.5). For each cat, pixels were assigned to one of five bins according to the strength of their direction selectivity. These bins correspond to the bars in the histogram in Fig. 5A. For each direction-selectivity bin, we calculated the relative area of cortical territory representing cardinal directions. At the lowest direction-selective domains, typically located around directional fractures, horizontal directions (Fig. 5B, black curves) were overrepresented compared to vertical directions (mean ± SEM, 54.9 ± 1.1 and 45.1 ± 1.1%, respectively; paired *t*-test, $P < 0.001$). As direction-selectivity increased, horizontal direction representation decreased. The

FIG. 3. Direction maps and distribution of preferred directions in the cat area 18. (A) Blood vessel patterns, direction preference map and direction selectivity map for the two hemispheres of one of the cats examined. For each direction preference map, we calculated the percentage of pixels that responded best to each cardinal direction. Strength of direction selectivity was computed on a scale from 0 to 1, with 1 corresponding to maximal selectivity (see Materials and methods). (B) Relative area of cortical territory representing cardinal directions (± SEM) in the 15 cats in which both hemispheres were recorded. Dark grey, light grey and black bins indicate pixels taken from the left, right and both hemispheres, respectively. ***$P < 0.001$ for the difference between the percentages of pixels representing the same direction between the two hemispheres. (C) Relative area of cortical territory representing cardinal directions (± SEM). Horizontal directions were classified with reference to the hemisphere as temporal or nasal. Each dot corresponds to a data point from each cat. Downward direction preferences were significantly overrepresented compared to all other directions ($P < 0.001$). Temporal directions were significantly overrepresented compared to nasal and upward directions ($P < 0.001$). Scale bars, 1 mm.

FIG. 4. Absence of orientation anisotropy. (A) Example of orientation preference map and direction preference map obtained from one cat (left hemisphere). (B) Scatter plots showing the relationship between orientation preference and direction preference for 1000 randomly chosen pixels. (C) Relative area of cortical territory representing cardinal and oblique orientations (± SEM).

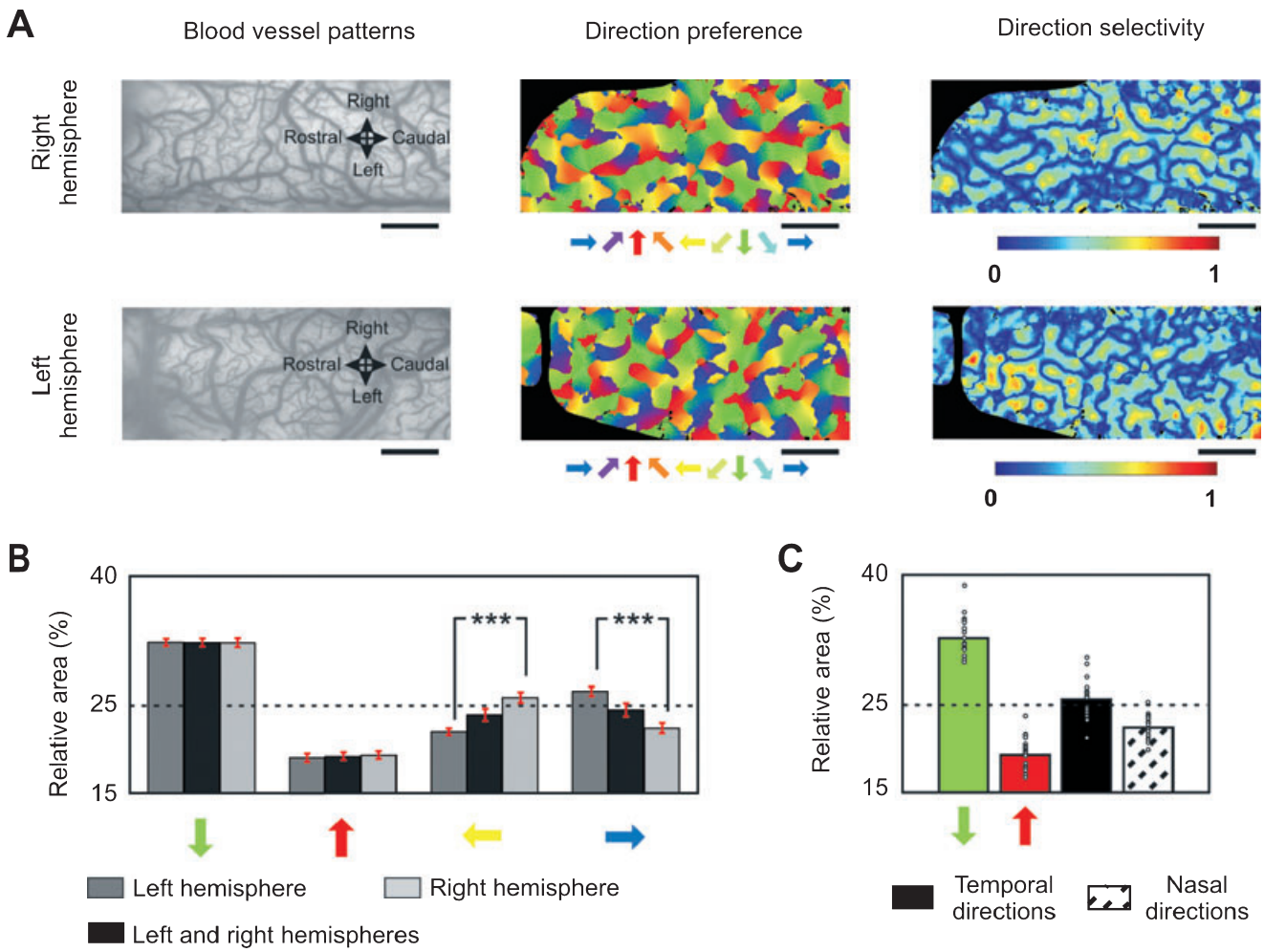

FIG. 3.

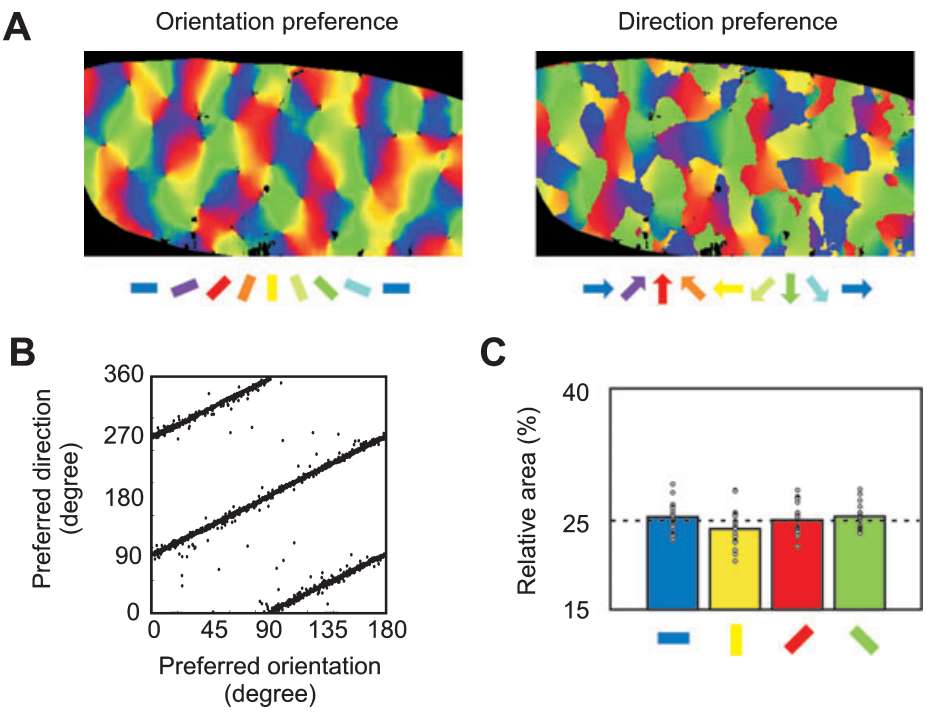

FIG. 4.

TABLE 1. Relative area of cortical territory representing cardinal directions obtained in 20 cats

Relative cortical territory area: preferred directions (%)					
Vertical directions		Lateral directions		ANOVA	
Downward	Upward	Temporal	Nasal	*F*-value	*P*-value
32.67 ± 0.48	19.32 ± 0.48	25.66 ± 0.49	22.43 ± 0.31	124.4	0.0001

Data are presented as percentage ± SEM. A one-way repeated-measures ANOVA was performed in each case in order to estimate the robustness of the anisotropy.

TABLE 2. Relative area of cortical territory representing cardinal and oblique orientations

Relative cortical territory are: preferred orientations (%)					
Cardinal orientations		Oblique orientations		ANOVA	
Horizontal	Vertical	45°	135°	*F*-value	*P*-value
25.42 ± 0.36	24.04 ± 0.50	25.07 ± 0.41	25.46 ± 0.30	2.02	0.12

Data are presented as percentage ± SEM. A one-way repeated-measures ANOVA was performed in each case in order to estimate the robustness of the anisotropy.

representation of the temporal directions (grey solid curve), however, remained larger than the representation of nasal directions (grey dashed curve).

Vertical directions exhibited a very different modulation with respect to direction selectivity. We found that downward directions (Fig. 5B, black solid curve) were significantly overrepresented (relative area > 25%) from bin 3 to bin 5 (one-group *t*-test, $P < 0.001$). In addition, the area of cortical territory representing downward directions was significantly larger than the area of cortical territory representing the three other cardinal directions at bin 4 and bin 5 (Bonferroni *post hoc* test, $P < 0.001$). Upward directions (Fig. 5B, black dashed curve), on the other hand, were underrepresented (relative area < 25%) at every direction selectivity bin (one-group *t*-test, $P < 0.001$ from bin 1 to bin 4, and $P < 0.05$ at bin 5). The overrepresentation of downward directions shown in Fig. 3C was therefore mainly attributable to pixels that exhibited the highest direction selectivity. In comparison, the overrepresentation of temporal directions was mainly attributable to pixels that exhibited the lowest direction selectivity.

Stimulation with randomly distributed dots

In order to check whether the nature of the stimuli could affect the calculation of the preferred direction, we performed one additional experiment with the use of randomly distributed dots moving in one direction. We compared the resulting single-condition maps with the single-condition maps obtained with the use of orientated moving gratings (Fig. 6A). The activity evoked by randomly distributed dots was much weaker than in the case of orientated moving gratings. However, some patterns with weak activity could be distinguished at the same regions that were activated with gratings. For each set of moving stimuli, we calculated the differential maps by subtracting the single-condition maps evoked by the stimulation with two opposite directions (Fig. 6B). The magnitude of the differential signal was

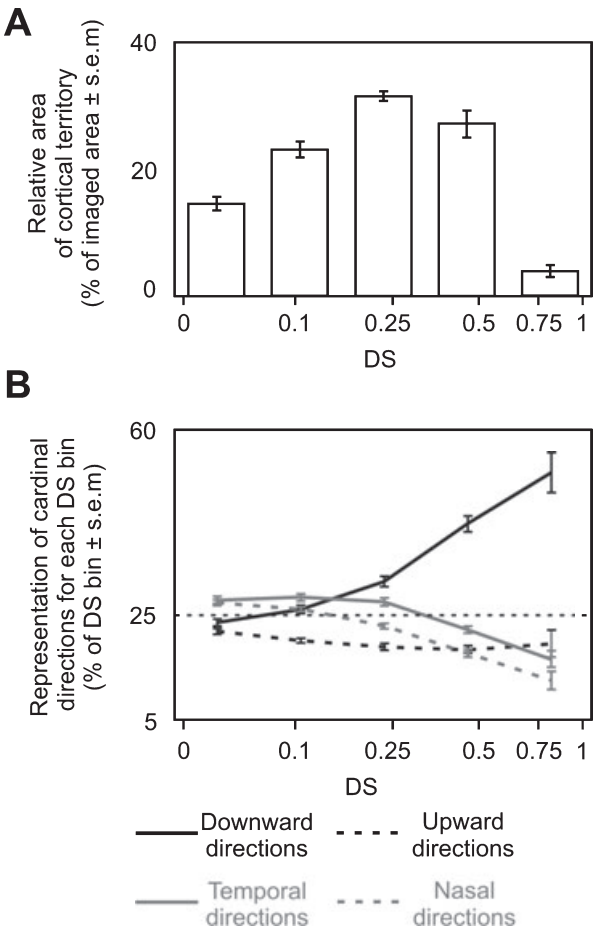

FIG. 5. Distribution of preferred directions and dependence on direction selectivity. (A) Average distribution of direction selectivity (± SEM). The representation is logarithmic. The lower and upper values of the five bins are: 0 and 0.065; 0.065 and 0.168; 0.168 and 0.331; 0.331 and 0.59; and 0.59 and 1. (B) Relative area of cortical territory representing cardinal directions (± SEM) for increasing direction-selectivity indices.

almost twice as weak in the case of randomly distributed dots. Despite this difference in response strength, the same columns were generally activated in both cases.

Discussion

Unlike area 17, area 18 receives geniculate input solely from the Y (magnocellular) pathway. Neurons in area 18 are more direction-selective (Orban *et al.*, 1981; McLean *et al.*, 1994). Area 18 is regarded as a critical stage in the cortical processing of motion signals (Pasternak & Maunsell, 1992). In this study, we examined the role of this area in the processing of self-motion. In the cat, higher cortical areas in cat visual cortex, such as lateral suprasylvian areas, appear to specialize in the processing of optic flows (Hamada, 1987; Rauschecker *et al.*, 1987; Sherk *et al.*, 1995; Brosseau-Lachaine *et al.*, 2001), yet area 18 is widely considered only to detect local components of motion, feeding higher visual areas for interpreting dynamic visual environment. We found that, even in area 18, there is an over-abundance of domains preferring downward and temporal directions in the central, lower visual field representation. These results are in accordance with the properties of the optic flow generated by forward locomotion, in which local directions of motion change with the location in the visual field.

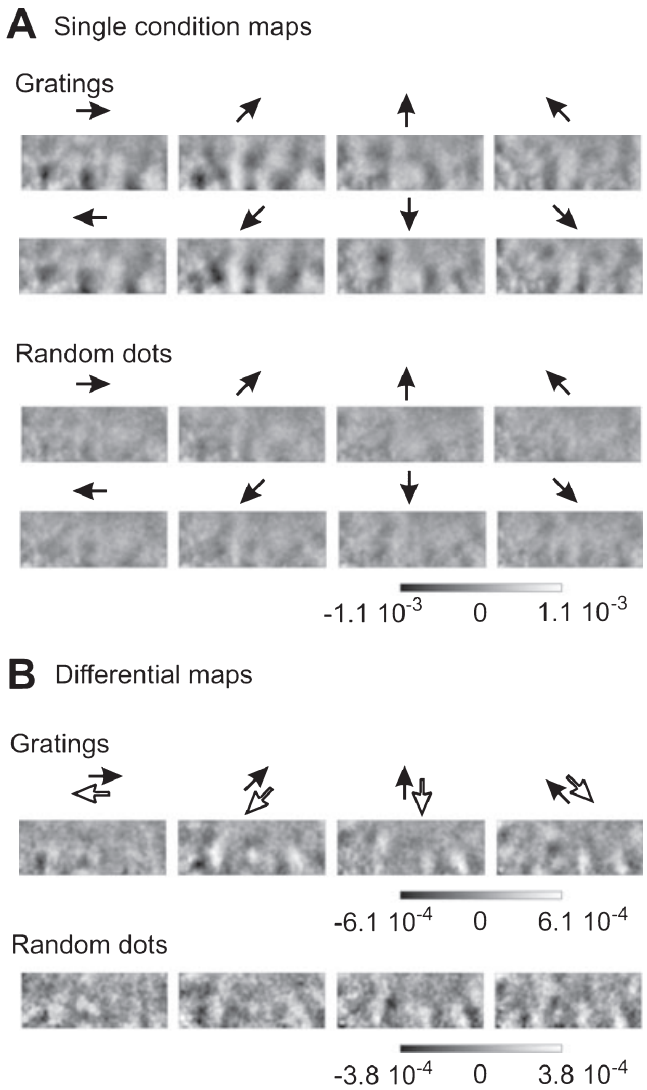

FIG. 6. Single-condition maps and direction maps evoked by two sets of stimulus pattern. One set was composed of orientated square-wave gratings, and the other set of randomly positioned dots. Each stimulus was moving in one direction. (A) Single-condition maps evoked by the two sets of stimuli for each direction. Gray scale shows response amplitude as fractional change in reflection. (B) Differential maps for pairs of opposite directions of motion evoked by the two sets of stimuli. Each differential map was reconstructed by subtracting a single-condition map in response to one direction of motion from a single-condition map in response to the opposite direction of motion. Dark and bright patches in each image represent cortical areas that preferred motion in the direction of the black and white arrows marked above the image, respectively. The full scale of grey levels was chosen according to each set of stimuli.

Relation with previous studies

Several studies based on electrophysiological recordings have pointed out an anisotropic representation of directions in cat area 18 (Berman *et al*., 1987; Bauer *et al*., 1989). Berman (1987) found that more neurons coded for downward and temporal directions than for the other directions. Moreover, they suggested that such anisotropy in direction representation can be partially explained by the overrepresentation of cardinal orientations compared to oblique ones. We did not find any significant overrepresentation of cardinal orientations (Table 2). This difference can be accounted for by the relatively advanced age of our cats, typically older than 11 weeks. At this age, cardinal orientations tend to be represented in area 18 equally to, or sometimes even more weakly, than oblique orientations (Coppola & White, 2004; Tani *et al*., 2006). Our results therefore support the idea that anisotropies for orientation and direction preferences are caused by different mechanisms.

Bauer *et al*. (1989) have also studied the representation of directions in cat area 18 with the use of stimuli composed of large randomly distributed dots, and found that upper-layer cells exhibited the overrepresentation of horizontal, mainly temporal, directions. Lower-layer cells, on the other hand, coded preferentially for vertical directions. We used orientated square-wave gratings and recorded the intrinsic signal originating mainly from the superficial layers of cat area 18. Although both studies emphasize the possible role of area 18 in the processing of self-motion through the overrepresentation of cardinal directions, it is difficult to reconcile their results with ours. The present study rather suggests that upper layers of cat area 18 exhibit the overrepresentation of both downward and temporal directions (Fig. 3C). One might want to interpret these differences in terms of differential responses to orientated gratings or randomly distributed dots (Shmuel & Grinvald, 1996; Galuske *et al*., 2002; for discussion see Swindale *et al*., 2003). Our data, however, support the idea that the same cortical columns are activated by both types of stimuli (Fig. 6). The discrepancy with the previous study might therefore not primarily arise from the choice of the stimulation pattern. Instead, their sample might be biased; this is much less likely to occur with optical imaging, in which thousands of pixels are recorded at the same time.

Role of direction selectivity

We investigated how cardinal directions were represented with respect to direction selectivity. Generally, direction selectivity values obtained with optical imaging of intrinsic signals (Fig. 5A) are rather weak compared to values obtained with unit recordings. These results are consistent with a previous study (Swindale *et al*., 2003) and certainly reflect the weaker columnar organization of direction selectivity compared to orientation preference or ocular dominance (DeAngelis *et al*., 1999). We found that downward direction representation increased with respect to direction selectivity (Fig. 5B). Temporal direction representation, on the other hand, decreased with respect to direction selectivity. Temporal direction representation was, however, significantly larger than nasal direction representation, except at the lowest direction selective domains.

During forward locomotion, the optic flow tends to direct left- and downward in the lower-left visual field and to direct right- and downward in the lower-right visual field (Gibson, 1954). The overrepresentation of downward and temporal directions is therefore in accordance with the expansion of the optic flow created by forward locomotion in each hemisphere. It remains, however, unclear why downward and temporal directions exhibit such a difference with respect to direction selectivity.

Acknowledgements

The authors would like to thank Katsuya Ozawa, Aya Iwashita, Yuji Akimoto and Toshiki Tani for their invaluable support to the authors' experiments.

References

Bauer, R., Hoffmann, K.P., Huber, H.P. & Mayr, M. (1989) Different anisotropies of movement direction in upper and lower layers of the cat's area 18 and their implications for global optic flow processing. *Exp. Brain Res.*, **74**, 395–401.

Berman, N.E., Wilkes, M.E. & Payne, B.R. (1987) Organization of orientation and direction selectivity in areas 17 and 18 of cat cerebral cortex. *J. Neurophysiol.*, **58**, 676–699.
Bishop, P.O., Kozak, W. & Vakkur, G.J. (1962) Some quantitative aspects of the cat's eye: axis and plane of reference, visual field co-ordinates and optics. *J. Physiol. (Lond.)*, **163**, 502.
Blasdel, G.G. & Salama, G. (1986) Voltage-sensitive dyes reveal a modular organization in monkey striate cortex. *Nature*, **321**, 579–585.
Bonhoeffer, T. & Grinvald, A. (1991) Iso-orientation domains in cat visual cortex are arranged in pinwheel-like patterns. *Nature*, **353**, 429–431.
Bonhoeffer, T. & Grinvald, A. (1996) Optical imaging based on intrinsic signals: the methodology. In Toga, A.W. & Mazziotta, J.C. (eds), *Brain Mapping: the Methods.* Academic Press, San Diego, pp 55–97.
Bonhoeffer, T., Kim, D.S., Malonek, D., Shoham, D. & Grinvald, A. (1995) Optical imaging of the layout of functional domains in area 17 and across the area 17/18 border in cat visual cortex. *Eur. J. Neurosci.*, **7**, 1973–1988.
Brosseau-Lachaine, O., Faubert, J. & Casanova, C. (2001) Functional sub-regions for optic flow processing in the posteromedial lateral suprasylvian cortex of the cat. *Cereb. Cortex*, **11**, 989–1001.
Coppola, D.M., Purves, H.R., McCoy, A.N. & Purves, D. (1998) The distribution of oriented contours in the real world. *Proc. Natl. Acad. Sci. USA*, **95**, 4002–4006.
Coppola, D.M. & White, L.E. (2004) Visual experience promotes the isotropic representation of orientation preference. *Vis. Neurosci.*, **21**, 39–51.
DeAngelis, G.C., Ghose, G.M., Ohzawa, I. & Freeman, R.D. (1999) Functional micro-organization of primary visual cortex: receptive field analysis of nearby neurons. *J. Neurosci.*, **19**, 4046–4064.
Frégnac, Y. & Imbert, M. (1978) Early development of visual cortical cells in normal and dark-reared kittens: relationship between orientation selectivity and ocular dominance. *J. Physiol. (Lond.)*, **278**, 27–44.
Galuske, R.A., Schmidt, K.E., Goebel, R., Lomber, S.G. & Payne, B.R. (2002) The role of feedback in shaping neural representations in cat visual cortex. *Proc. Natl. Acad. Sci. USA*, **99**, 17083–17088.
Gibson, J.J. (1954) The visual perception of objective motion and subjective movement. *Psychol. Rev.*, **61**, 304–314.
Hamada, T. (1987) Neural response to the motion of textures in the lateral suprasylvian area of cats. *Behav. Brain Res.*, **25**, 175–185.
Imamura, K., Tanaka, S., Ribot, J., Kobayashi, M., Yamamoto, M., Nakadate, K. & Watanabe, Y. (2006) Preservation of functional architecture in visual cortex of cats with experimentally induced hydrocephalus. *Eur. J. Neurosci.*, **23**, 2087–2098.
Koenderink, J.J. (1986) Optic flow. *Vision Res.*, **26**, 161–180.
McLean, J., Raab, S. & Palmer, L.A. (1994) Contribution of linear mechanisms to the specification of local motion by simple cells in areas 17 and 18 of the cat. *Vis. Neurosci.*, **11**, 271–294.
Movshon, J.A., Thompson, I.D. & Tolhurst, D.J. (1978) Spatial and temporal contrast sensitivity of neurones in areas 17 and 18 of the cat's visual cortex. *J. Physiol. (Lond.)*, **283**, 101–120.
Orban, G.A., Kennedy, H. & Maes, H. (1981) Response to movement of neurons in areas 17 and 18 of the cat: direction selectivity. *J. Neurophysiol.*, **45**, 1059–1073.
Pasternak, T. & Maunsell, J.H. (1992) Spatiotemporal sensitivity following lesions of area 18 in the cat. *J. Neurosci.*, **12**, 4521–4529.
Rauschecker, J.P., von Grunau, M.W. & Poulin, C. (1987) Centrifugal organization of direction preferences in the cat's lateral suprasylvian visual cortex and its relation to flow field processing. *J. Neurosci.*, **7**, 943–958.
Sherk, H. & Fowler, G.A. (2001) Neural analysis of visual information during locomotion. *Prog. Brain Res.*, **134**, 247–264.
Sherk, H., Kim, J.N. & Mulligan, K. (1995) Neuronal responses in extrastriate cortex to objects in optic flow fields. *Vis. Neurosci.*, **12**, 887–894.
Shmuel, A. & Grinvald, A. (1996) Functional organization for direction of motion and its relationship to orientation maps in cat area 18. *J. Neurosci.*, **16**, 6945–6964.
Swindale, N.V., Grinvald, A. & Shmuel, A. (2003) The spatial pattern of response magnitude and selectivity for orientation and direction in cat visual cortex. *Cereb. Cortex*, **13**, 225–238.
Swindale, N.V., Matsubara, J.A. & Cynader, M.S. (1987) Surface organization of orientation and direction selectivity in cat area 18. *J. Neurosci.*, **7**, 1414–1427.
Tani, T., Ribot, J. & Tanaka, S. (2006) Effect of visual experience on orientation map development for different spatial frequencies. *Soc. Neurosci. Abstr.*, 619.4/B42.
Tusa, R.J., Rosenquist, A.C. & Palmer, L.A. (1979) Retinotopic organization of areas 18 and 19 in the cat. *J. Comp. Neurol.*, **185**, 657–678.
Wang, G. (2004) Functional segregation of plural regions representing cardinal contours in cat primary visual cortex. *Eur. J. Neurosci.*, **20**, 1906–1914.
Weliky, M., Bosking, W.H. & Fitzpatrick, D. (1996) A systematic map of direction preference in primary visual cortex. *Nature*, **379**, 725–728.
Yokoo, T., Knight, B.W. & Sirovich, L. (2001) An optimization approach to signal extraction from noisy multivariate data. *Neuroimage*, **14**, 1309–1326.